

## Supplementary Material

# Nearly hollow Ru-Cu-MoO<sub>2</sub> octahedrons consisting of clusters and nanocrystals for high efficiency hydrogen evolution reaction

Qian Liu<sup>a,b</sup>, Chengtian Zhang<sup>a</sup>, Pengyan Wang<sup>a</sup>, Ding Chen<sup>a</sup>, Manjie Xiao<sup>a</sup>, Lei Chen<sup>a</sup>,  
Suli Liu<sup>c</sup>, Jun Yu<sup>a,b</sup>, Shichun Mu<sup>a,b\*</sup>

a. *State Key Laboratory of Advanced Technology for Materials Synthesis and Processing, Wuhan University of Technology, Wuhan 430070, China.*

b. *Foshan Xianhu Laboratory of the Advanced Energy Science and Technology Guangdong Laboratory, Xianhu hydrogen Valley, Foshan 528200, China.*

c. *Key Laboratory of Advanced Functional Materials of Nanjing, Nanjing Xiaozhuang University, Nanjing 211171, Jiangsu, China*

\* Corresponding author E-mail: [msc@whut.edu.cn](mailto:msc@whut.edu.cn); [niuniu\\_410@126.com](mailto:niuniu_410@126.com)

### **Materials and reagent.**

Cupric acetate monohydrate ( $((\text{CH}_3\text{COO})_2\text{Cu}\cdot\text{H}_2\text{O})$ ), L-glutamic acid ( $\text{C}_5\text{H}_9\text{NO}_4$ ) and absolute ethanol were purchased from Sinopharm Chemical Reagents, China. Phosphomolybdic acid were from Shanghai Macklin Biochemical Co., Ltd. 1,3,5-benzenetricarboxylic acid ( $\text{H}_3\text{BTC}$ ) and ruthenium chloride hydrate ( $\text{RuCl}_3\cdot x\text{H}_2\text{O}$ ) were obtained from Aladdin Reagents Ltd.  $\text{RuO}_2$ , Pt/C (20 wt %) and Nafion (5 wt %) were purchased from Sigma-Aldrich. All chemicals used in experiment were analytical grade and have not been further purified. The deionized water used in the whole experiment was ultrapure water (18.25 M $\Omega$ ).

### **Preparation of NENU-5.**

In a typical procedure, 0.6 g of copper (II) acetate monohydrate ( $((\text{CH}_3\text{COO})_2\text{Cu}\cdot\text{H}_2\text{O})$ ) 220 mg of L-glutamic acid and 0.9 g of phosphomolybdic acid hydrate were mixed in 120 ml of deionized water with stirring at ambient condition for 30 min. And then, 422 mg of  $\text{H}_3\text{BTC}$  were dissolved in 120 ml of ethanol, which was swiftly injected into the above solution in succession. Then, the resulting solution was stirred for 14 h at room temperature. The precipitate was obtained by centrifugation and washed twice with ethanol. Then the NENU-5 powders were dried in vacuum at 70 °C overnight.

### **Material Characterization.**

The phase structure and crystal structure of the catalyst were characterized by Empyrean Type X-ray diffraction instrument using Cu  $K\alpha$  as radiation source. The XPS spectrum was acquired by ESCALAB 250Xi X-ray photoelectron spectrometer with Al  $K\alpha$  as excitation source. The morphology and structure were obtained by scanning

electron microscopy (SEM, Zeiss Ultra Plus) and transmission electron microscopy (TEM, Talos F200S). The X-ray spectroscopy (EDS) analysis were performed on a Talos F200S as well.

### **Preparation the working electrode.**

A catalyst-ink was prepared for as-prepared samples by ultra-sonic dispersion of 5.0 mg of catalyst in a solution of 20  $\mu\text{L}$  Nafion, 500  $\mu\text{L}$  water and 500  $\mu\text{L}$  ethyl alcohol. The working electrode with the loading of 0.714  $\text{mg cm}^{-2}$  was prepared by loading the catalyst-ink (10  $\mu\text{L}$ ) onto a glassy carbon electrode (0.07  $\text{cm}^2$ ). For comparison, 5 mg commercial catalyst powder (20 wt% Pt/C) was evenly dispersed into the same mixture, then 10  $\mu\text{L}$  ink was loaded onto the GC electrode with the same mass loading.

### **Electrochemical Measurements.**

All electrochemical measurements in this paper were made by Shanghai Chenhua Electrochemical Workstation (CHI660E). Under alkaline condition and alkaline seawater media, Hg/HgO was used as reference electrode and graphite rod as counter electrode to form a traditional three-electrode system.  $E(\text{vs. RHE}) = E(\text{vs. Hg/HgO}) + 0.0591 \times \text{pH} + 0.098 \text{ V}$ . Seawater was obtained from the Yellow Sea, China's Huang Hai. To prepare the alkaline seawater media, the collected seawater was first filtered to remove the insoluble impurities. Then, the potassium hydroxide was added into the seawater to obtain the 1 M KOH solution. After stirring for 0.5 h, the solution was filtered again to remove the precipitated substances. The obtained 1M KOH aqueous solution and alkaline seawater solution were used as the electrolytes. Under acidic conditions, we selected Ag/AgCl as the reference electrode and the corresponding

potential was obtained from the following equation:  $E$  (vs. RHE) =  $E$  (vs. Ag/AgCl) +  $0.0591 \times \text{pH} + 0.098$  V. In addition, the LSV curves of HER employed the scan rate of  $5 \text{ mV s}^{-1}$ . and the polarization curves were plotted by the formula:  $E_{\text{actual}} = E_{\text{test}} - iR_s \times 100\%$ . The electrochemical impedance spectroscopy (EIS) was conducted at the corresponding potentials of  $10 \text{ mA cm}^{-2}$  from LSV curves, with the frequency range of 0.1 Hz to 100kHz and the AC amplitude of 10 mV. The overpotentials from the  $i$ - $t$  curve in 1 M KOH, 0.5 M  $\text{H}_2\text{SO}_4$  and seawater are 30, 64 and 38 mV, respectively. The hydrogen gas was collected by the water drainage method. A constant potential was applied on the electrode and the volume of evolved gases was recorded synchronously. Then the volume of  $\text{H}_2$  were calculated based on the gas laws. The theoretically expected volume of  $\text{H}_2$  was then calculated by applying the Faraday law, which states that the passage of 96500 C causes 1 equivalent of reaction.

### **Density Functional Theory (DFT) Calculation.**

DFT calculations in this work were performed using the CASTEP module in Materials Studio. The projected augmented wave (PAW) method was utilized to describe the electron-ion interactions. The generalized gradient approximation (GGA) with the Perdew-Burke-Ernzerhof (PBE) was employed to describe the electron exchange and correlation interactions. The Monkhorst-Pack grid  $k$ -points of  $3 \times 3 \times 1$  were employed to integrate the Brillouin zone. The custom energy cutoff and self-consistent field (SCF) tolerance were set to 400 eV and  $1.0 \times 10^{-5}$  eV/atom, respectively. The Cu (111) and  $\text{MoO}_2$  (011) crystal planes were adopted for theoretical calculations. The Cu- $\text{MoO}_2$  interface was constructed by adjusting the arrangement between two surfaces. For the

HER in alkaline solution, both the water dissociation and the hydrogen adsorption were considered. The total energies for H<sub>2</sub>O adsorption were calculated as follows:

$$\Delta E_{\text{H}_2\text{O}} = E(\text{H}_2\text{O}^*) - E(^*) - E(\text{H}_2\text{O})$$

Similarly, the Gibbs free energy of H adsorption was calculated as follows:

$$\Delta G_{\text{H}^*} = \Delta E_{\text{H}^*} + \Delta \text{ZPE} - T\Delta S = E(\text{H}^*) - E(^*) - E(\text{H}_2)/2 + \Delta \text{ZPE} - T\Delta S$$

Where  $\Delta \text{ZPE}$  is the zero-point energy and  $T\Delta S$  stands for the entropy corrections.

According to the previous report by Norskov et al., we used the 0.24 eV for the  $\Delta \text{ZPE} - T\Delta S$  of hydrogen adsorption in this work.

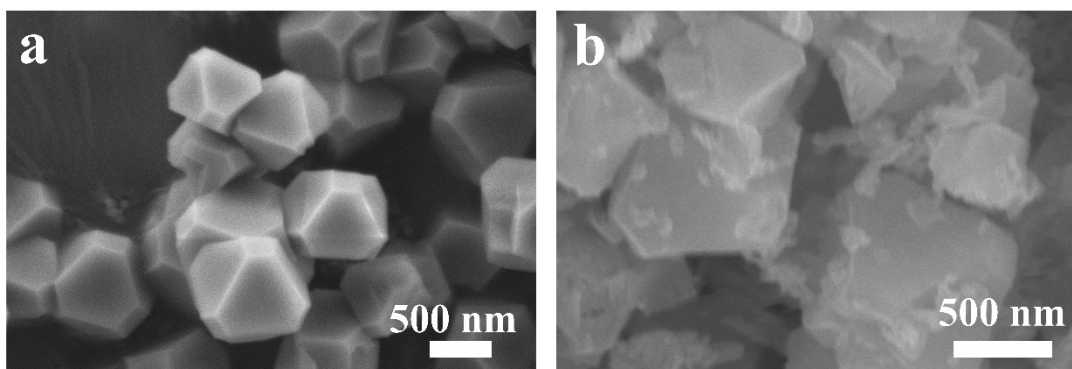


**Figure S1.** SEM image of (a) NENU-5 and (b) Ru-NENU-5.

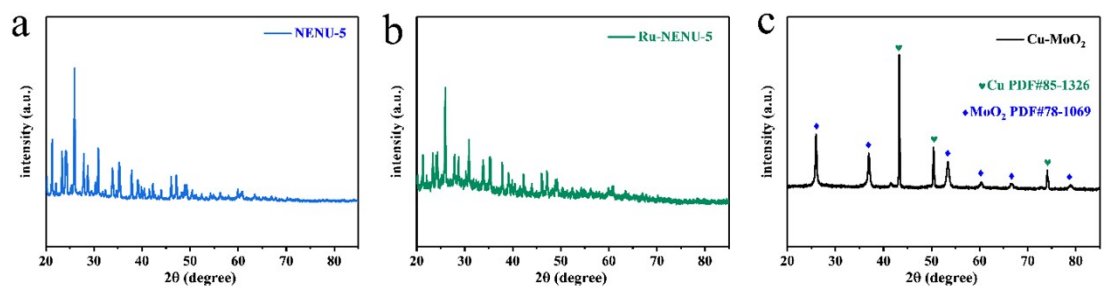


**Figure S2.** XRD pattern of (a) NENU-5 (b) Ru-NENU-5 and (c) Cu-MoO<sub>2</sub>.

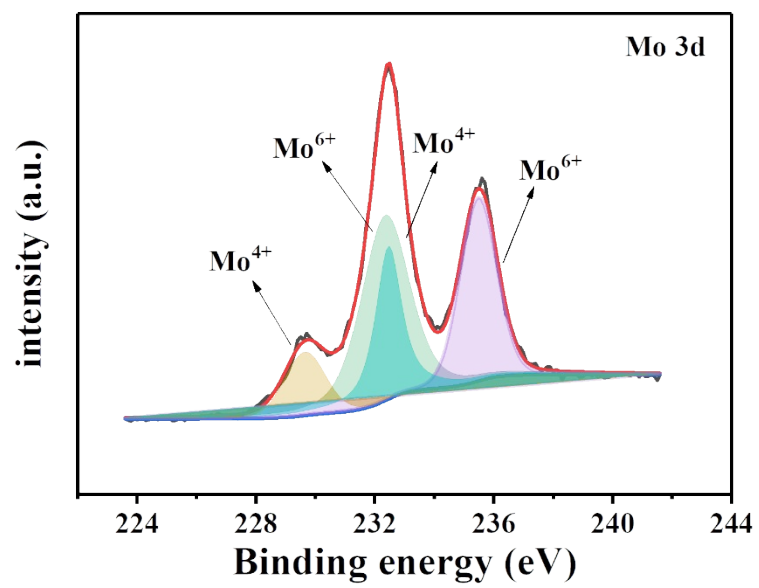


**Figure S3.** XPS spectrum of Ru-Cu-MoO<sub>2</sub>-48h.

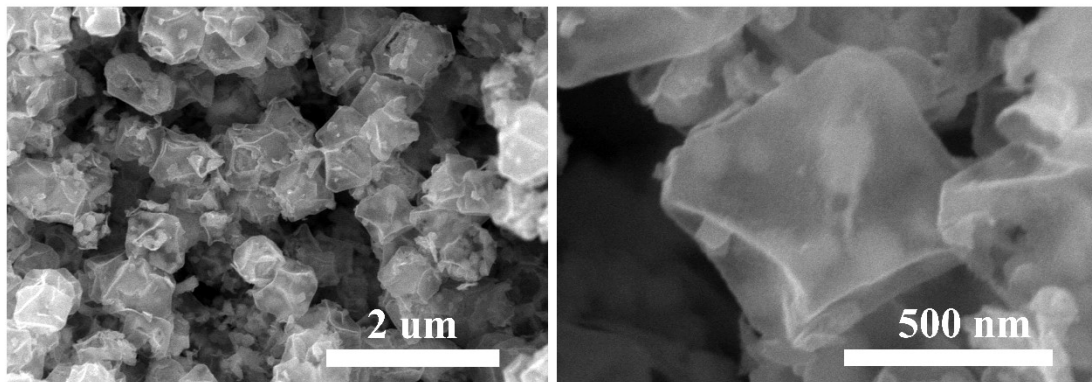


**Figure S4.** SEM image of Ru-Cu-MoO<sub>2</sub>-48h.

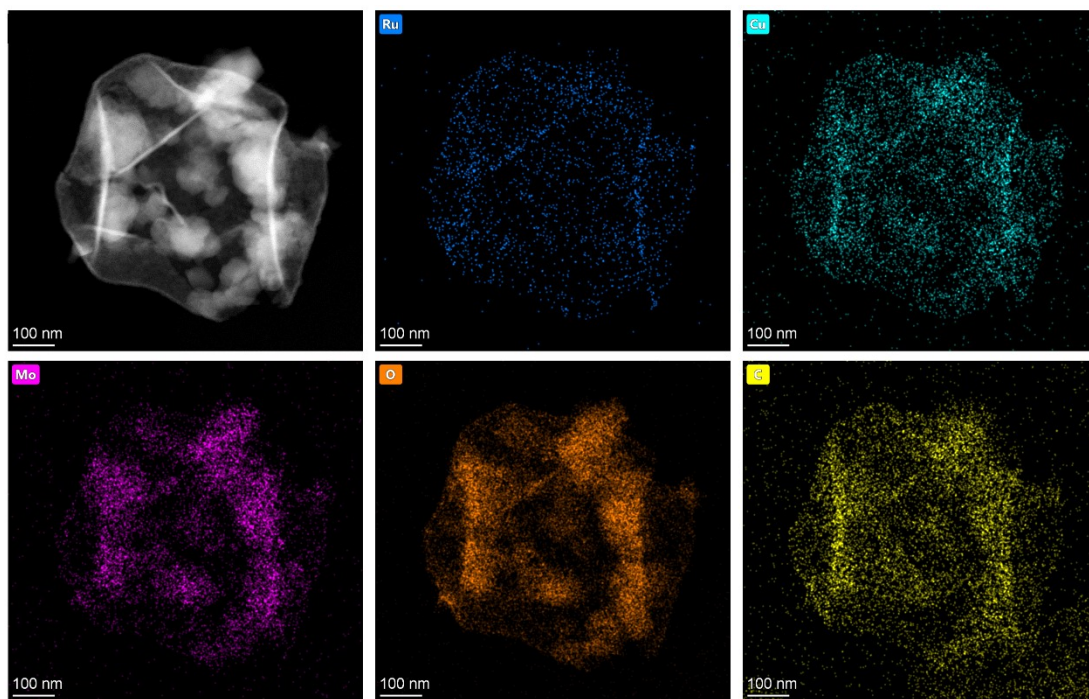


**Figure S5.** HADF-STEM image and EDS mapping of Ru-Cu-MoO<sub>2</sub>-48h

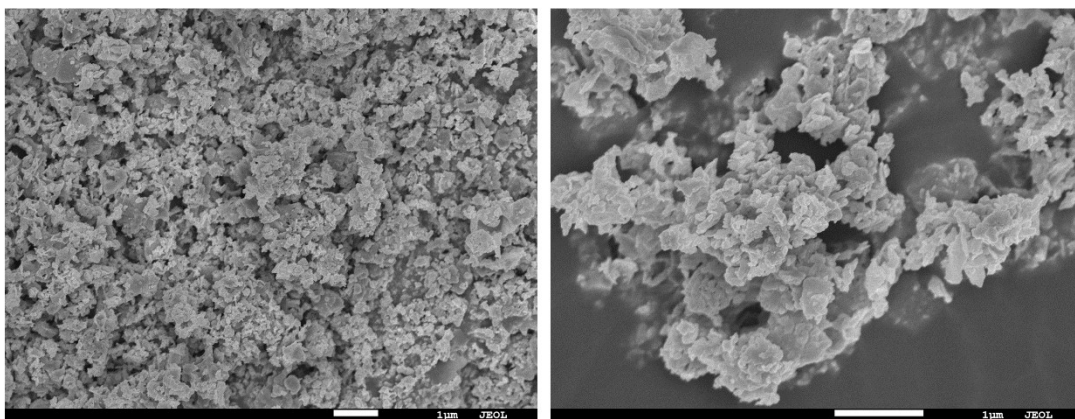


**Figure S6.** SEM image of Ru-Cu-MoO<sub>2</sub>-96h.

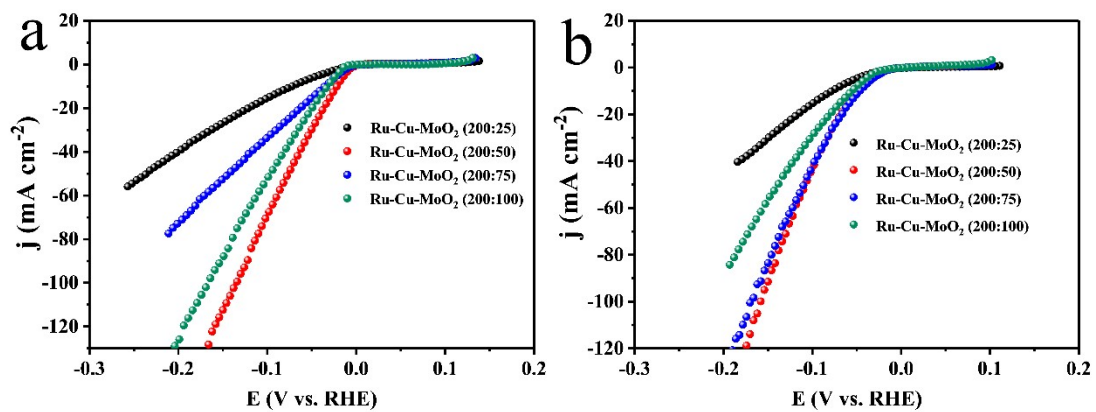


**Figure S7.** HER performance of Ru-Cu-MoO<sub>2</sub>-48h with different proportions in (a) 1 M KOH and (b) 0.5 M H<sub>2</sub>SO<sub>4</sub>.

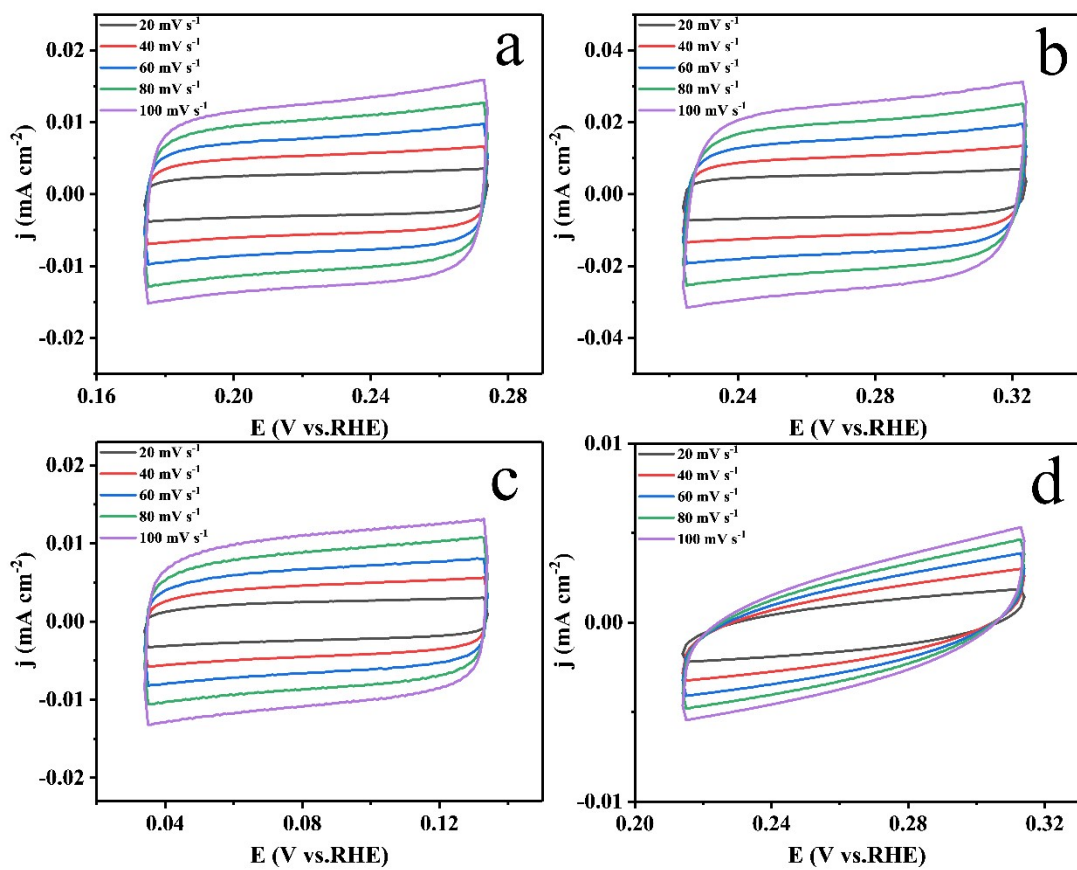


**Figure S8.** CV test of (a) Ru-Cu-MoO<sub>2</sub>-24h, (b) Ru-Cu-MoO<sub>2</sub>-48h, Ru-Cu-MoO<sub>2</sub>-96h and (d) Cu-MoO<sub>2</sub> in 1 M KOH.

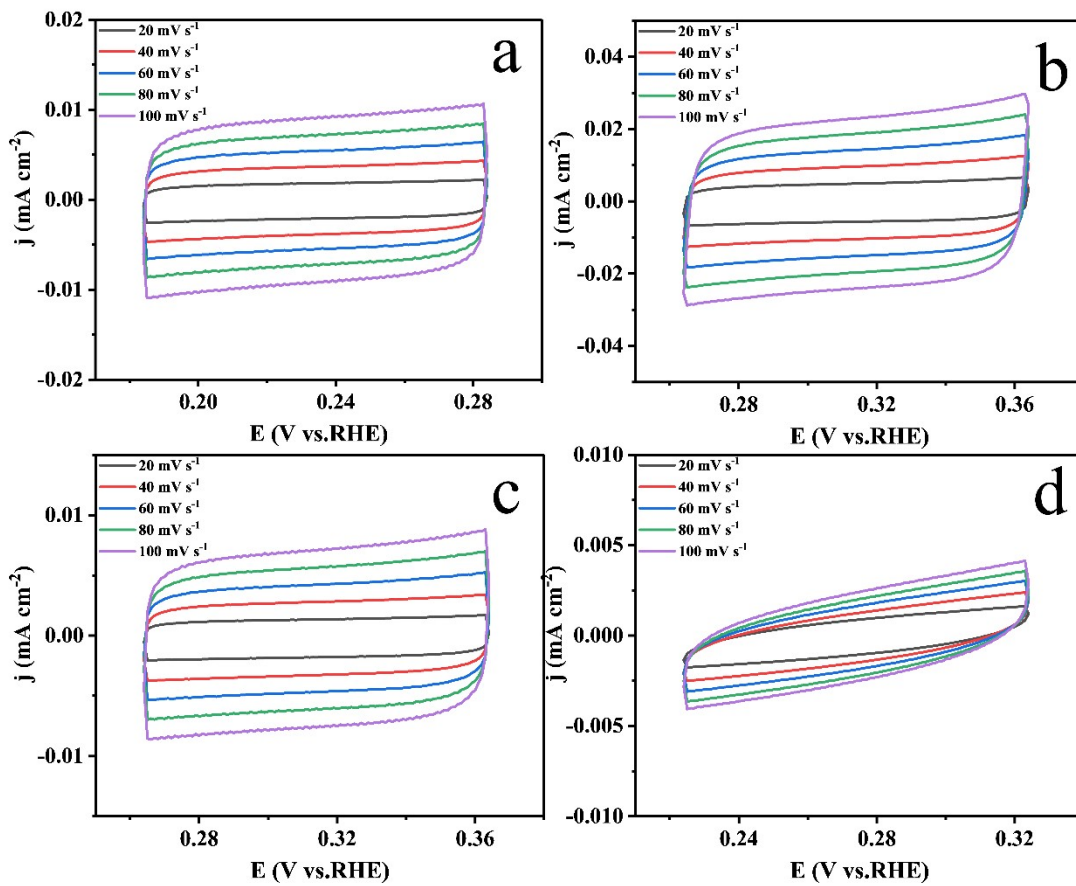


**Figure S9.** CV test of (a) Ru-Cu-MoO<sub>2</sub>-24h, (b) Ru-Cu-MoO<sub>2</sub>-48h, Ru-Cu-MoO<sub>2</sub>-96h and (d) Cu-MoO<sub>2</sub> in 0.5 M H<sub>2</sub>SO<sub>4</sub>.

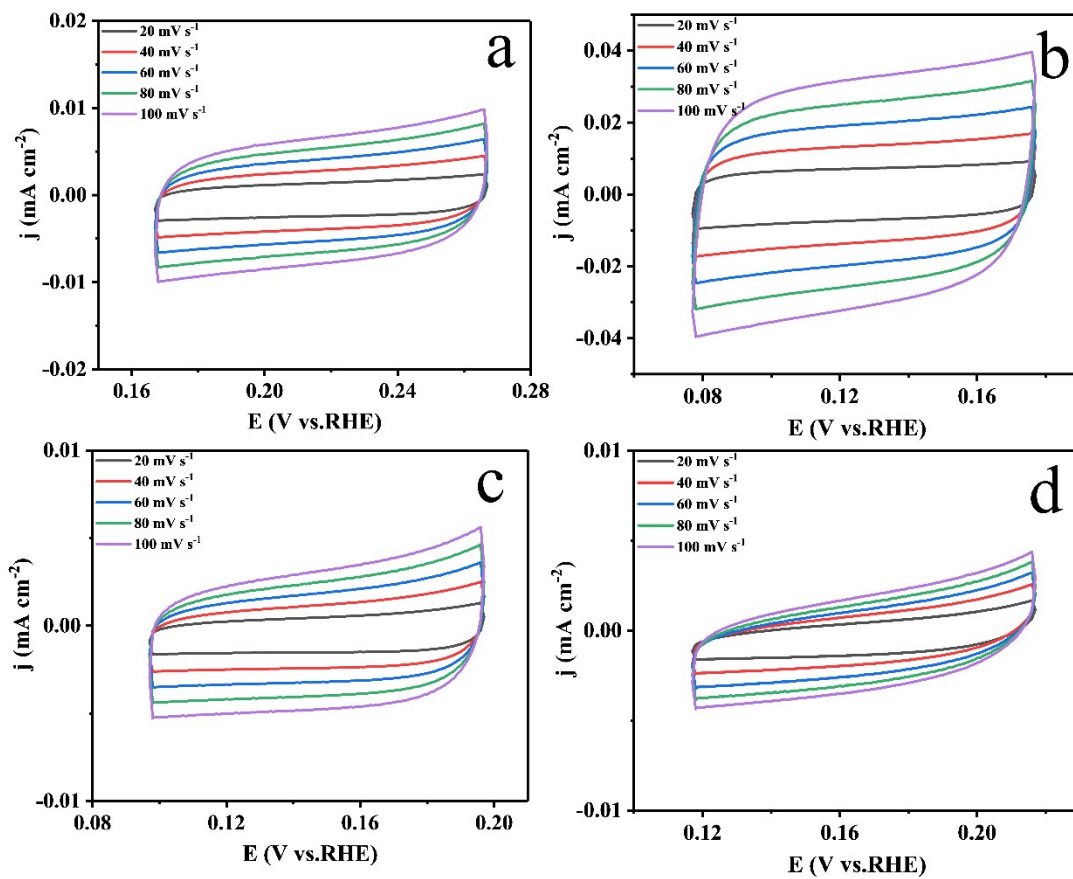


**Figure S10.** CV test of (a) Ru-Cu-MoO<sub>2</sub>-24h, (b) Ru-Cu-MoO<sub>2</sub>-48h, Ru-Cu-MoO<sub>2</sub>-96h and (d) Cu-MoO<sub>2</sub> in alkaline seawater.

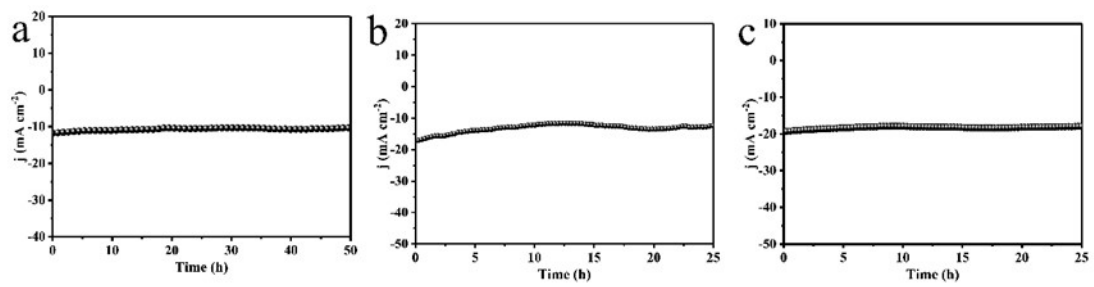


**Figure S11.** Time-reliant current density curve for Ru-Cu-MoO<sub>2</sub>-48h (a) in 1 M KOH.

(b) in 0.5 M H<sub>2</sub>SO<sub>4</sub> (c) in seawater.

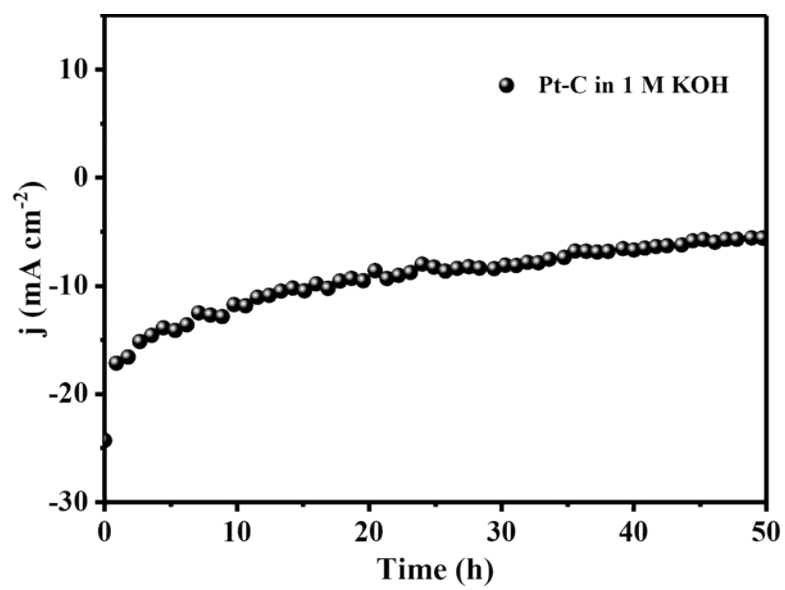


**Figure S12.** Long-term durability tests of Pt/C in 1 M KOH

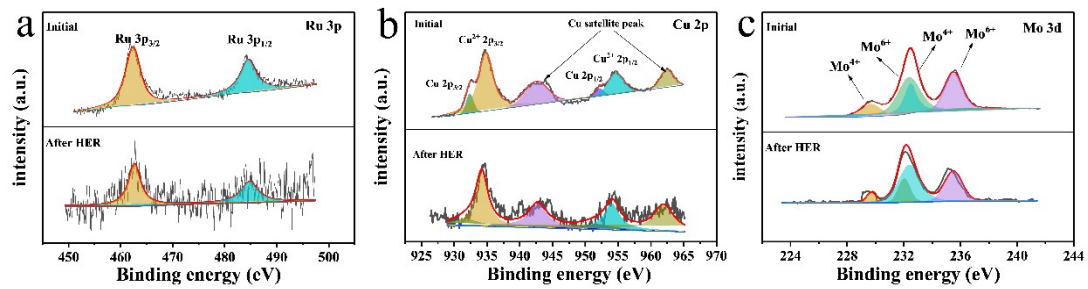


**Figure S13.** (a) XPS spectrum of Ru-Cu-MoO<sub>2</sub>-48h (a) Ru (b) Cu and (c) Mo before and after HER test.

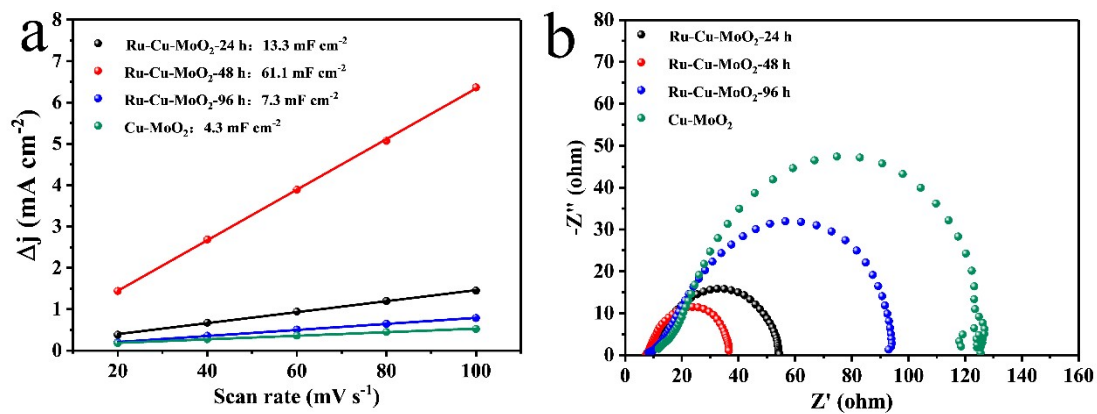


**Figure S14.** (a)  $C_{dl}$  in 0.5 M H<sub>2</sub>SO<sub>4</sub>. (b) Nyquist plots in 0.5 M H<sub>2</sub>SO<sub>4</sub>.

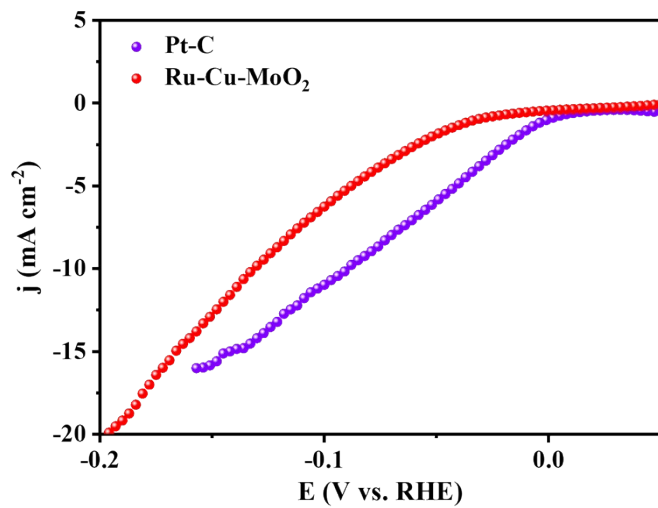


**Figure S15.** Polarization curves of Ru-Cu-MoO<sub>2</sub>-48h in 1M PBS

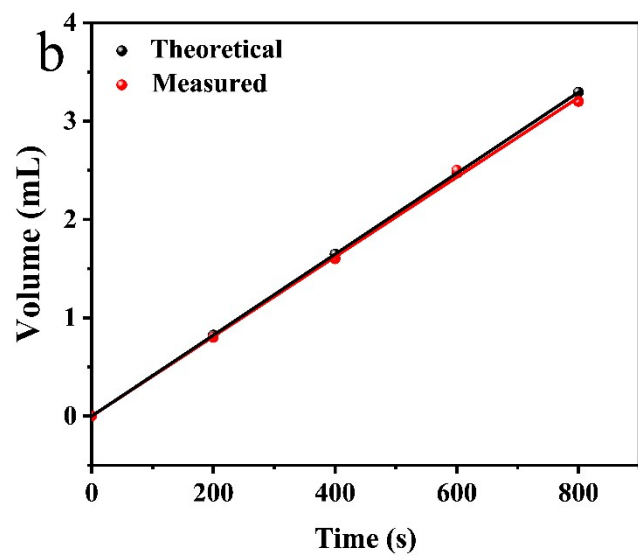


**Figure S16.** (a) Amount of  $H_2$  generation experimentally measured in 1 M KOH. (b)

Electrocatalytic efficiency of  $H_2$  generation over Ru-Cu-MoO<sub>2</sub> in 1 M KOH.

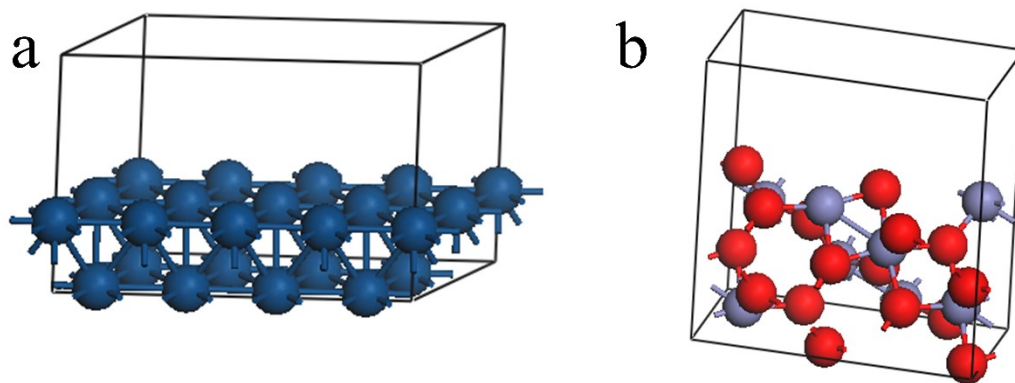


**Figure S17.** Structure models of (a) Cu and (b) MoO<sub>2</sub>.

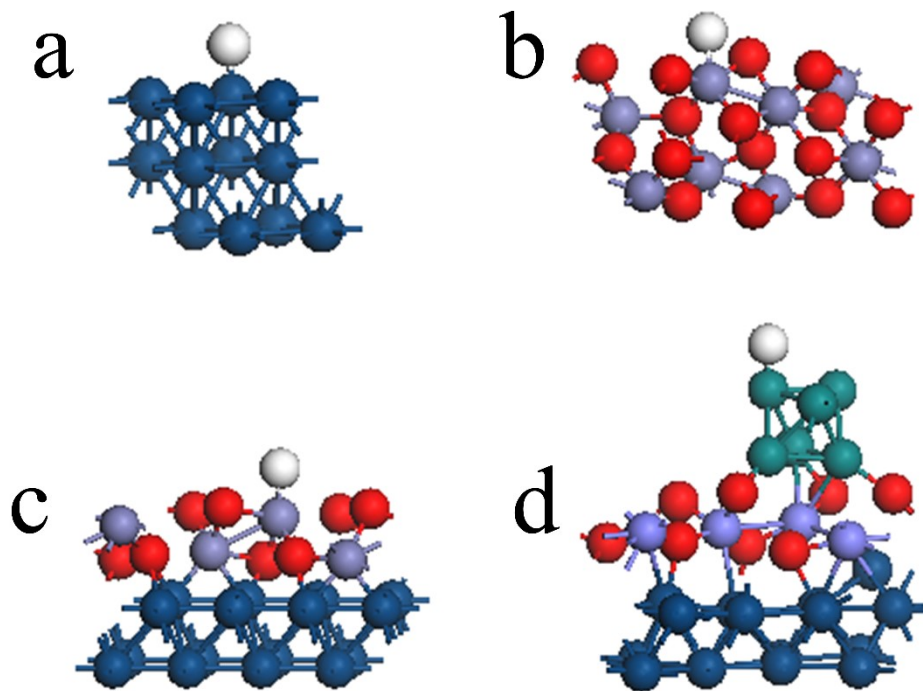


**Figure S18.** Structure models of hydrogen adsorption (a) Cu and (b) MoO<sub>2</sub> (c) Cu-MoO<sub>2</sub> and (d) Ru-Cu-MoO<sub>2</sub>.

**Table S1** The contents of Ru, Cu and Mo of Ru-Cu-MoO<sub>2</sub>-24h, Ru-Cu-MoO<sub>2</sub>-48h and Ru-Cu-MoO<sub>2</sub>-96h

<b>Catalyst</b>	<b>The content of Ru(wt)</b>	<b>The content of Cu(wt)</b>	<b>The content of Mo(wt)</b>
Ru-Cu-MoO <sub>2</sub> -24h	10.69%	22.77%	32.16%
Ru-Cu-MoO <sub>2</sub> -48h	14.39%	21.50%	30.89%
Ru-Cu-MoO <sub>2</sub> -96h	45.71%	22.65%	34.84

**Table S2** Comparison of HER performance in acidic media and alkaline media for the Ru-Cu-MoO<sub>2</sub> and other electrocatalysts

Catalyst	electrolyte	Overpotential @j(mV @ mA cm <sup>-2</sup> )	Tafel slope (mV dec <sup>-1</sup> )	Ref.
Ru-Cu-MoO <sub>2</sub>	1 M KOH	22@10	35	This work
	0.5M H <sub>2</sub> SO <sub>4</sub>	48@10	60	
Ru-MoO <sub>2</sub>	1 M KOH	29@10	31	1
	0.5M H <sub>2</sub> SO <sub>4</sub>	55@10	44	
2D-	1 M KOH	25@10	33	2
MoO <sub>2</sub> /Ru/NC	0.5M H <sub>2</sub> SO <sub>4</sub>	68@10	38	
hcp-Ru@NC	0.5M H <sub>2</sub> SO <sub>4</sub>	27.5@10	33	3
Mo <sub>2</sub> C@Ru	0.5M H <sub>2</sub> SO <sub>4</sub>	24.6@10	--	4
Ru-Mo <sub>2</sub> C/CN	1 M KOH	34@10	80	5
ECM@Ru	0.5M H <sub>2</sub> SO <sub>4</sub>	63@10	47	6
Ru/Co <sub>3</sub> O <sub>4</sub> NW	1 M KOH	31@10	69.75	7
Ru@CDs	1 M KOH	30@10	22	8
Ru-OCNT	1 M KOH	34@10	27.8	9
	0.5M H <sub>2</sub> SO <sub>4</sub>	55@10	36	
Ru-Co <sub>3</sub> O <sub>4</sub> - NiO-NF	1 M KOH	44@10	53.9	10
Ru@NC	1 M KOH	29@10	27	11

	0.5M H <sub>2</sub> SO <sub>4</sub>	62@10	40	
Ru <sub>x</sub> Se@MoS <sub>2</sub>	1 M KOH	45@10	42.9	12
	0.5M H <sub>2</sub> SO <sub>4</sub>	120@10	72.2	
Ru-NG	1 M KOH	25.9@10	32.6	13
Ru/Ni <sub>2</sub> P@NPC	1 M KOH	89@10	124	14
	0.5M H <sub>2</sub> SO <sub>4</sub>	132@10	62	

---

## Reference

1. P. Jiang, Y. Yang, R. Shi, G. Xia, J. Chen, J. Su and Q. Chen, *J. Mater. Chem. A*, 2017, **5**, 5475-5485.
2. N. Yuan, Q. Jiang, Z. Wu and J. Tang, *J. Phys. Chem. C*, 2020, **124**, 10804-10814.
3. Y. Li, L. A. Zhang, Y. Qin, F. Chu, Y. Kong, Y. Tao, Y. Li, Y. Bu, D. Ding and M. Liu, *ACS Catal.*, 2018, **8**, 5714-5720.
4. Z. Zhang, P. Li, Q. Feng, B. Wei, C. Deng, J. Fan, H. Li and H. Wang, *ACS Appl. Mater. Interfaces*, 2018, **10**, 32171-32179.
5. J. Chen, C. Chen, Y. Chen, H. Wang, S. Mao and Y. Wang, *J. Catal.*, 2020, **392**, 313-321.
6. H. Zhang, W. Zhou, X. F. Lu, T. Chen and X. W. Lou, *Adv. Energy Mater.*, 2020, **10**, 2000882.
7. Z. Liu, L. Zeng, J. Yu, L. Yang, J. Zhang, X. Zhang, F. Han, L. Zhao, X. Li, H. Liu and W. Zhou, *Nano Energy*, 2021, **85**, 105940.
8. Z. Liu, B. Li, Y. Feng, D. Jia, C. Li, Q. Sun and Y. Zhou, *Small*, 2021, **17**, 2102496.
9. R. Ding, L. Lin, C. Pei, X. Yu, Q. Sun and H. S. Park, *Chem. Eur. J.*, 2021, **27**,

11150-11157.

10. H. Zhang, H. Guo, J. Ren, X. Jin, X. Li and R. Song, *Chem. Eng. J.*, 2021, **426**, 131300.

11. B. Zheng, L. Ma, B. Li, D. Chen, X. Li, J. He, J. Xie, M. Robert and T.-C. Lau, *Catal. Sci. Technol.*, 2020, **10**, 4405-4411.

12. Q. Chen, K. Wang, J. Qin, S. Wang, W. Wei, J. Wang, Q. Shen, P. Qu and D. Liu, *RSC Adv.*, 2019, **9**, 13486-13493.

13. Y. Li, Y. Luo, Z. Zhang, Q. Yu, C. Li, Q. Zhang, Z. Zheng, H. Liu, B. Liu and S. Dou, *Carbon*, 2021, **183**, 362-367.

14. J.-Q. Chi, X.-Y. Zhang, X. Ma, B. Dong, J.-Q. Zhang, B.-Y. Guo, M. Yang, L. Wang, Y.-M. Chai and C. Liu, *ACS Sustain. Chem. Eng.*, 2019, **7**, 17714-17722.